Nanoscale Advances

ROYAL SOCIETY OF CHEMISTRY

PAPER

View Article Online
View Journal

Cite this: DOI: 10.1039/d5na01052g

Bioengineered Ag/AgCl nanoparticles from *Kocuria kristinae*: sustainable synthesis with potent antibacterial, hepatotoxic, and enzyme-modulating activities

Lana Mohammed,[a] Mohsin A. Salih,[b] Zana H. Ibrahim,[c] Payam B. Hassan,[d] Sameera Sh. Mohammad Ameen,[e] Khalid M. Omer,*[f] Zhinya Y. Majeed,[a] Dalya M. Hamad,[a] Shnyar O. Ahmed,[a] Rayan F. Hassan[a] and Hevy N. Hussein[a]

In response to the growing threat of multidrug-resistant microorganisms, there is an urgent necessity for developing eco-friendly synthesis methods for the generation of nanoparticles that can serve efficiently as alternatives to commercial antibacterial agents. In spite of the achievement in this area, their toxicity remains insufficiently explored, underscoring the necessity for detailed toxicological evaluation. Herein, Ag/AgCl nanoparticles were generated *via* a green biosynthetic approach, where metabolites excreted by the soil-isolated bacterium *Kocuria kristinae* served as both reducing and stabilizing agents during nanoparticle formation. The resulting nanoparticles were stable, spherical, and had an average size of 40 ± 10 nm, as confirmed by TEM analysis. Their stability was further indicated by a high negative zeta potential of −45.8 mV. Ag/AgCl-NPs showed excellent antibacterial effectiveness against pathogenic *S. aureus*, *P. aeruginosa*, *A. baumannii*, and *E. coli* ATCC 25922, with an MIC of 7 μg mL^{-1}, 7 μg mL^{-1}, 10 μg mL^{-1}, and 8 μg mL^{-1}, respectively. Furthermore, the hepatotoxic effects of the biofabricated Ag/AgCl-NPs were evaluated histopathologically and enzymatically in mature male albino rats following intraperitoneal injection of a low dose (10 mg kg^{-1}) and a high dose (20 mg kg^{-1}) of Ag/AgCl-NPs. The findings indicated minor to moderate liver toxicity, characterized by steatosis, tissue degradation including necrosis, and hyperplasia of Kupffer cells, according to the dose administered. Nonetheless, liver metabolism and function may be slightly affected, as levels of liver enzymes AST and ALT were considerably reduced ($p < 0.05$), whereas only ALP showed a significant increase ($p < 0.05$) in the low-dose nanoparticle-treated group. Thus, the biofabricated Ag/AgCl-NPs can serve as effective bactericidal agents with low to moderate hepatic effects and minimal alteration in liver functioning.

Received 12th November 2025
Accepted 20th March 2026

DOI: 10.1039/d5na01052g

rsc.li/nanoscale-advances

1 Introduction

The excessive and improper use of antibiotics in this era resulted in the emergence of resistant bacteria, including multidrug-resistant (MDR) strains, which are resistant to many different drugs and cause serious health issues. This topic is presently one of the world's significant issues, particularly with nosocomial strains isolated from hospitals, which can induce infections necessitating complex and demanding treatment.[1] Gram-negative, non-motile, glucose non-fermenting pathogens *Acinetobacter baumannii* and *Pseudomonas aeruginosa* are the most prominent MDR opportunistic bacteria being reported and found.[2,3] They effectively acclimate to the hospital environment, making them the primary pathogens responsible for nosocomial infections. These microorganisms possess the capability to develop resistance to a broad spectrum of antibiotics through diverse mechanisms, consequently leading to life-threatening infections.[4,5] *A. baumannii* infections in patients with serious illnesses include ventilator-associated pneumonia, bloodstream infections, wound infections, and nosocomial meningitis.[6] Moreover, nosocomial *P. aeruginosa* is the predominant Gram-negative pathogen responsible for infections in burn-wound patients, urinary tract infections and it has been associated with blood stream infections and mortality.[7,8]

[a]*Department of Medical Laboratory, College of Health and Medical Technology, Sulaimani Polytechnic University, Sulaymaniyah, Kurdistan region, Iraq*

[b]*Department of Nursing, College of Health and Medical Technology, Sulaimani Polytechnic University, Sulaymaniyah, Kurdistan region, Iraq*

[c]*Department of Medical Laboratory Science, College of Science, University of Raparin, Ranya, Sulaymaniyah, Iraq*

[d]*Department of Biology, College of Science, University of Sulaimani, Qliasan St., 46002, Sulaymaniyah, Kurdistan region, Iraq*

[e]*Department of Chemistry, College of Science, University of Zakho, 42002, Zakho, Kurdistan region, Iraq*

[f]*Department of Chemistry, College of Science, University of Sulaimani, Qliasan St., 46002, Sulaymaniyah, Kurdistan region, Iraq. E-mail: Khalid.omer@univsul.edu.iq*

This bacterium accounts for 10–20% of ventilator-associated pneumonia cases, coming after *Staphylococcus aureus*.[9] *Staphylococcus aureus* is a commensal Gram-positive bacterium that inhabits human skin and the upper respiratory tract, prevalent in 30% of the general population, and is regarded as a globally life-threatening pathogen.[10] Soft tissue infections, bacteremia, endocarditis, pneumonia, toxemic syndromes, and food poisoning, are among the infections that this bacterium can cause.[11–13] Hospital-acquired *S. aureus*, especially methicillin-resistant strains, constitutes a significant source of nosocomial infections associated with elevated mortality and morbidity rates.[14] All referenced pathogens are members of the MDR ESKAPE group of pathogens, which include *Enterococcus faecium*, *S. aureus*, *Klebsiella pneumoniae*, *A. baumannii*, *P. aeruginosa*, and *Enterobacter* spp. The WHO categorizes these bacteria as a MDR and critical group of pathogens that urgently require novel antibiotics in clinical settings.[15] Consequently, identifying novel pharmacological targets and developing innovative treatments for these pathogens is essential to address this issue and improve human health.

Recently, many types of nanomaterials including nanocomposites, carbon-based materials, and MOFs have been developed for diverse applications in energy, sensing, environmental remediation, and biomedicine.[16–25] Numerous metal elements readily interact with oxygen under various conditions, leading to the formation of metal oxides with different structural architectures.[26,27] Metallic nanoparticles have garnered interest as a potentially viable alternative therapeutic agent for addressing the MDR issue due to their high surface area-to-volume ratio and distinctive physicochemical features.[28] Research indicates that silver and silver chloride nanoparticles (AgNPs and AgCl-NPs) exhibit superior efficacy in inhibiting the growth and causing the eradication of pathogenic microbes associated with certain common human disorders.[29–39] Chemical and physical approaches for the fabrication of nanoparticles present challenges in terms of nanoparticle shape and size management and releasing toxic residual materials.[40–44] To overcome the limitations of these approaches, the application of biological methods has emerged as a viable alternative that was found to be simple, cost-effective, reliable, environmentally friendly, and biocompatible.[45–47] Using bacterial metabolites for the synthesis of metallic nanoparticles offers several advantages, as the process is eco-friendly by avoiding toxic chemicals, biocompatible due to reduced toxicity, and cost-effective since it relies on naturally occurring byproducts instead of expensive reagents.[48] It is also energy-efficient, typically occurring under mild conditions without the need for high energy input. Additionally, metabolites such as proteins, enzymes, and polysaccharides act as capping agents that enhance nanoparticle stability and prevent aggregation.[49] This method is highly scalable because bacteria can be easily cultured in large volumes, and it provides functionalization potential, with metabolites imparting added biological activities such as antimicrobial or antioxidant properties.

Notwithstanding the extensive benefits of Ag/AgCl-NPs, apprehension exists regarding the possible harmful consequences of these nanoparticles in healthy human cells, akin to those seen in microbial cells.[50,51] Various types of nanoparticles are known to mostly accumulate in the liver tissue upon entering the body, establishing it as a principal site for initial interactions and potential negative consequences. This preferred buildup results from the liver's role in detoxifying and blood filtration.[52,53] Therefore, a comprehensive assessment of the toxicity of green-synthesized nanoparticles that can be used as an antimicrobial agent is essential to guarantee their safe implementation in various future biomedical applications.

Kocuria species are Gram-positive, non-motile, non-spore-forming, coccoid bacteria that are catalase-positive and coagulase-negative, classified within the family Micrococcaceae, order Actinomycetales, and class Actinobacteria. This genus consists of around 18 species, which can be described as diploids, tetrads, or irregular clusters.[54,55] *Kocuria kristinae* is present on human skin, mucosal surfaces, and in soil. *K. kristinae* is considered a benign cutaneous bacterium; however, there are cases of infections associated with it in immunosuppressed people.[56–58] Research on the biosynthesis of nanoparticles from the *Kocuria* species is limited. It has been reported that silver nanoparticles have been synthesized from the external metabolites of *Kocuria rosea* and *Kocuria* sp.[59,60]

The present study focuses on the extracellular biosynthesis of silver/silver chloride nanoparticles (Ag/AgCl-NPs) utilizing metabolites produced by *K. kristinae*, aiming to explore their effectiveness as antibacterial agents against clinically significant MDR pathogens, namely *A. baumannii*, *P. aeruginosa*, and *S. aureus*. To the best of our knowledge, this is the first study reporting the green synthesis of Ag/AgCl-NPs using metabolites from soil-isolated *K. kristinae*. Unlike previous studies that produce only AgNPs, our approach yields Ag/AgCl hybrid nanoparticles and provides a comprehensive biological evaluation. Beyond determining their antimicrobial potential, the present investigation also addresses safety concerns by examining the possible toxicological effects of the biosynthesized nanoparticles on mammalian systems (Fig. 1). To achieve this, hepatotoxicity was evaluated in albino rats through both biochemical assays and histological analyses of liver tissue, providing insight into how exposure to Ag/AgCl-NPs may impact vital organ function and structure. This dual approach not only highlights the therapeutic promise of biogenically synthesized Ag/AgCl-NPs but also underscores the importance of assessing their biocompatibility before biomedical application.

2 Materials and methods

2.1 *Kocuria kristinae* isolation and identification

A soil sample was collected from Sulaimani Polytechnic University, thereafter diluted in a saline solution (0.9% NaCl), and inoculated into nutrient agar plates. The plates were subsequently positioned in an incubator at 37 °C for 48 hours to facilitate the growth of distinct bacterial colonies. The isolated bacteria were evaluated for their ability to synthesize Ag/AgCl-NPs. Among all examined bacteria, the isolate *K. kristinae* showed the most remarkable capacity for Ag/AgCl-NP synthesis, as indicated by the notable color transition of the mixture (comprising bacterial metabolite and $AgNO_3$) from yellow to

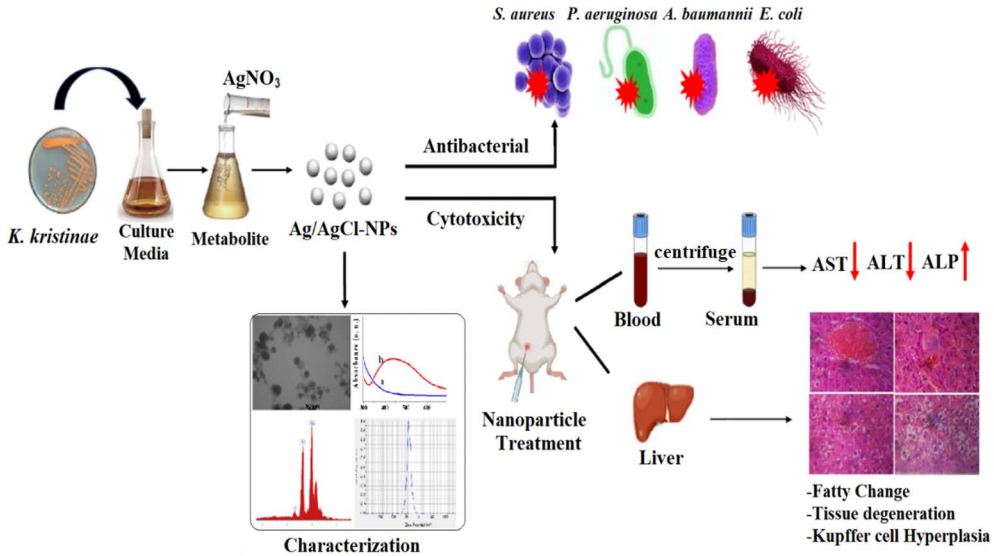

Fig. 1 Schematic diagram showing the preparation of Ag/AgCl nanoparticles, along with their characterization and biomedical applications.

brown within a few minutes. A Vitek 2 automated system was utilized to determine the genus and species of the isolate. The outcome of this analysis verified that the bacterial isolate is *K. kristinae* with a 99% level of certainty (Fig. S1).

2.2 Biosynthesis of Ag/AgCl nanoparticles

Nanoparticles of Ag/AgCl were prepared following the procedure of Mohammed *et al.*[61] with minor modifications. The bacterium *K. kristinae* was cultured in 500 mL of nutrient broth and incubated at 37 °C for 48 hours in a shaker incubator set to 150 rpm. The culture underwent filtration using Whatman No. 1 filter paper with a pore size of 11 μm, after which the supernatant was mixed with an $AgNO_3$ solution (2 mM)in a 1 : 1 ratio (v/v) and incubated at room temperature for 24 to 48 hours. The synthesized Ag/AgCl-NPs were collected *via* high-speed centrifugation at 14 000 rpm for 20 minutes, and subsequently, washing with distilled water (1 : 1 v/v) was carried out to remove unreacted residues. The pure nanoparticles were subsequently powdered following air-drying at 40 °C in a hot air oven for a duration of 24 to 48 hours. Furthermore, the bacterial supernatant and silver nitrate solution were employed as controls.

2.3 Characterization of Ag/AgCl nanoparticles

The process of bio-reduction of Ag^+ ions was observed using a UV-visible spectrum and measured with a UV-vis spectrophotometer (Agilent Cary 60, USA) over the wavelength range of 200 to 700 nanometers. X-ray diffraction (XRD) was recorded to check the presence, crystalline nature, and phase variety of the synthesized Ag/AgCl-NPs. The analysis was conducted using a Cu-Kα radiation source within a scattering range (2θ) of 20–70° (Pan Analytical, X-pert Pro, Netherlands). Energy dispersive X-ray spectroscopy (Bruker, Germany) was used to examine the elemental composition of the produced nanoparticles. The size, shape, and morphology of the biosynthesized Ag/AgCl-NPs were analyzed using transmission electron microscopy (JEOL, JEM-2100, Japan). In order to determine the potential stability of the biosynthesized colloidal Ag/AgCl-NPs, the magnitude of the electrostatic charge potential at the electrical double layer encircling the biosynthesized Ag/AgCl-NPs was measured using a Zetasizer instrument (Horiba Jobin Jyovin Sz100, Vietnam).

2.4 Minimum inhibition concentration

The microtiter plate assay was used to determine the minimum inhibitory concentration (MIC) of Ag/AgCl-NPs against pathogenic MDR bacteria *S. aureus*, *P. aeruginosa*, *A. baumanni*, and *E. coli* ATCC 25922 as outlined by Mohammed *et al.*[61] Briefly, Ag/AgCl-NPs were synthesized at different concentrations from 1 to 12 μg mL^{-1}. In a 96-well plate, 100 μL of an overnight cultured microbial suspension (1×10^6 CFU mL^{-1}) was treated with 100 μL of Ag/AgCl-NPs at different concentrations. The plate was incubated at 37 °C for 18 to 24 hours, after which the absorbance of each well was measured at a wavelength of 595 nm.

2.5 Hepatotoxicity effect of Ag/AgCl NPs on albino rats

2.5.1. Laboratory animals. Eighteen male albino rats (*Rattus norvegicus*) weighing around 180–200 g were utilized. The experiment was conducted between November 2024 and December 2024 in the animal facility of the Medical Laboratory Science Department at Raparin University, College of Science. The animals were housed in plastic cages lined with wood chips, maintained at a regulated temperature of 22 ± 4 °C, subjected to 12-hour light/dark cycles, and provided with regular meals and drink *ad libitum*. All animal procedures were performed in accordance with the Guidelines for Care and Use of Laboratory Animals of the Medical Laboratory Science Department at Raparin University, College of Science, and approved by the Animal Ethics Committee of the Medical

Laboratory Science Department at Raparin University, College of Science.

2.5.2. Acute toxicity study. In an acute toxicity study, 12-hour fasted animals ($n = 12$) were randomly selected and divided into two groups of six rats each. High and low doses of Ag/AgCl-NPs (20 and 10 mg kg^{-1} BW, respectively) were administered intraperitoneally. The animals underwent continuous examination for 3 hours, after which any overnight mortality was recorded.

2.5.3. Experimental design. Rats were assigned to three groups at random ($n = 6$). Group I: Normal Control (NC). The group was administered a standard rat diet and distilled water for a duration of two weeks. Group II: Low Dose Nanoparticle (LDNP). The group was administered Ag/AgCl-NPs (10 mg kg^{-1} BW) intraperitoneally every 72 hours for a duration of 2 weeks. Group III: High-Dose Nanoparticle (HDNP). The group was administered Ag/AgCl-NPs (20 mg kg^{-1} BW) intraperitoneally every 72 hours for a duration of 2 weeks. At the conclusion of the study period (48 hours post-injection of the final nanoparticle dose), the animals were subjected to overnight fasting and subsequently anaesthetized intraperitoneally using a ketamine–xylazine combination (90 mg kg^{-1} and 10 mg kg^{-1}).[62] Cardiac blood samples were obtained and allowed to clot. Serum was obtained through centrifugation at 2500 rpm for 15 minutes and subsequently analysed for various biochemical parameters. In addition, liver organs were excised, rinsed with normal saline, and preserved in 10% formalin for histopathological analysis.

2.5.4. Measurement of serum parameters. Serum concentrations of aspartate aminotransferase (AST), alanine aminotransferase (ALT), and alkaline phosphatase (ALP) were measured using a fully automated analyzer (Cobas e-411, Roche Diagnostics, Switzerland).

2.5.5. Histopathological study. The histopathological study was based on the procedure established by Hussein and Ibrahim.[63] Briefly, sections of liver tissue from both Ag/AgCl-NP-treated and untreated rats were preserved in 10% neutral formalin and subsequently analysed for pathological evidence of hepatotoxicity. Tissue samples in the laboratory underwent standard histological processing. The tissue sections stained with hematoxylin and eosin were analysed at 400× magnification using a light microscope, and the analysis was conducted with AmScope software. The degree of lipid alterations, hepatic degeneration, and Kupffer cell activity was semi-quantitatively evaluated in all experimental groups. The circular area of hepatocytes exhibiting fatty alterations was quantified in square microns (μm^2) across ten randomly selected locations on each slide. Only lipid-accumulated regions within larger hepatocytes were quantified, eliminating nuclei and unoccupied cytoplasm. The proportion of fatty degeneration was determined using the formula:

$$\text{Fatty changes } \% = (\text{fatty area within hepatocytes} \div \text{total hepatocyte area}) \times 100$$

The total tissue area indicative of hepatic degeneration was quantified in μm^2 at 400× magnification across 10 fields per slide. Regions of deteriorated tissue, encompassing necrosis and fibrosis, were quantified within identical fields. The degeneration % was calculated using the formula:

$$\text{Percentage of degeneration } (\%) = (\text{degenerated area} \div \text{total tissue area}) \times 100$$

To assess Kupffer cell activity, chronic inflammatory cells were enumerated in 10 distinct fields per slide within groups demonstrating Kupffer cell hyperplasia. The average quantity of inflammatory cells per group was computed to assess the level of inflammation. The histological modification in the Ag/AgCl-NP treated liver tissue was scored and staged as summarized in Table 1.

Table 1 Score evaluation for hepatic histopathological lesions

Lesions	Interpretation	Score	Grade
Fatty change	Absence	0	No
	<%35 of hepatocytes	1	Mild
	%35–75 of hepatocytes	2	Moderate
	>%75 of hepatocytes	3	Severe
Degeneration	Absence	0	No
	<%25 degenerated area	1	Mild
	%25–50 degenerated area	2	Moderate
	>%50 degenerated area	3	Severe
Inflammation	Absence	0	No
	<%10 Kuffer cell hyperplasia	1	Mild
	%10–25 Kuffer cell hyperplasia	2	Moderate
	>%25 Kuffer cell hyperplasia	3	Severe

2.6 Statistical analysis

Data were analyzed using GraphPad Prism (Version 8.0.2). The results are expressed as mean ± standard error (mean ± SE). Each experimental group comprised six rats ($n = 6$). Biochemical assays were conducted with a minimum of five replicates for each sample. Statistical differences were determined by the Dunnett-test for multiple comparisons after analysis of variance (ANOVA). The level of significance was fixed at $P < 0.05$.

3 Results and discussion

3.1 Isolation and identification of used bacteria

K. kristinae was isolated from soil for the synthesis of Ag/AgCl-NPs. The MDR bacteria including, *S. aureus*, *P. aeruginosa*, and *A. baumannii* were obtained from Smart Hospital, and *E. coli* ATCC 25922 was obtained from the Biology laboratory at Sulaimani Polytechnic University. All used bacteria were identified through the Vitek 2 automated system (Fig. S2–S4).

3.2 Synthesis of Ag/AgCl nanoparticles

Many biological agents, including bacteria, fungi, and plants, have been used to synthesize nanoparticles in an eco-friendly way.[64] We utilized the *K. kristinae* supernatant (metabolites) to synthesize Ag/AgCl-NPs in our experiment as an eco-friendly approach. The reduction of Ag^+ to elemental silver (Ag^0) was

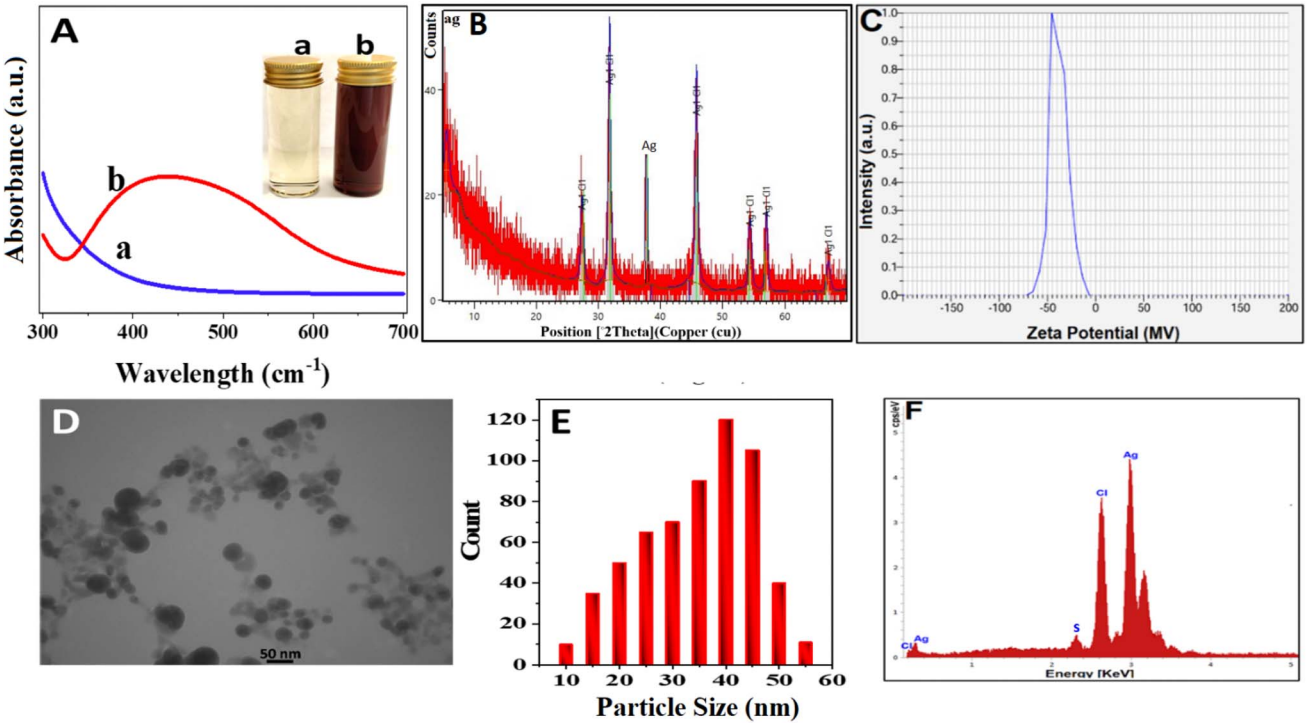

Fig. 2 Characterization of biosynthesized Ag/AgCl-NPs. (A) UV-vis spectroscopy; (B) XRD spectrum; (C) zeta potential; (D) TEM micrograph; (E) Ag/AgCl-NP size distribution histogram; (F) EDX analysis.

evidenced by a noticeable color change in the reaction mixture, confirming the successful synthesis of silver nanoparticles (Ag-NPs). Upon the addition of $AgNO_3$ to the bacterial supernatant, the solution gradually transformed from colorless to pale yellow and then to dark brown, a characteristic indication of plasmonic Ag nanoparticle formation (Fig. 2A, inset). In our study, we propose that Ag/AgCl-NPs are also generated (as confirmed by PXRD and EDX analysis), likely due to the presence of chloride ions naturally present in the culture media of *K. kristinae*, which facilitate the formation of Ag/AgCl along with elemental silver. Similar results were noticed in other published reports in the literature.[65,66] This observation suggests that the bacterial metabolites not only reduce silver ions but also contribute to the nucleation and stabilization of AgCl-NPs.

3.3 Characterization of Ag/AgCl nanoparticles

The confirmation of extracellular biosynthesis of Ag/AgCl-NPs was carried out first using UV-vis spectroscopy (Fig. 2A). The UV-visible absorption spectra of Ag/AgCl-NPs were obtained at a wavelength of 420 nm. Conversely, the control tube containing just the bacterial supernatant did not display any absorption peaks at the specified wavelengths, as illustrated in Fig. 2A. It has been reported that the presence of surface plasmon resonance within the wavelength range of 350–500 nm generally indicates the formation of small, spherical Ag/AgCl-NPs.[67] The crystalline structure of the synthesized nanoparticles was examined using XRD analysis. The XRD spectrum of the dried nanoparticle powder displayed sharp diffraction peaks in the 2θ range of 20° to 70° at 27.91°, 32.32°, 46.27°, 54.85°, 57.49°, and 67.42°, which correspond to the (111), (200), (220), (311), (222), and (400) planes of the face-centered cubic structure of Ag/AgCl-NP crystals, and were indexed as silver chloride. Notably, some of these peaks overlap with or are similar to those characteristic of metallic silver (Ag) nanoparticles, indicating the presence of both Ag and AgCl phases. Therefore, the XRD results suggest that the synthesized product is a composite mixture of Ag/AgCl nanoparticles (Fig. 2B). Analogous findings were documented in other literature studies.[68,69] Moreover, the biosynthesized Ag/AgCl-NP solution exhibited a zeta potential of −45.8 mV, characterized by the presence of a singular peak that signifies repulsion among the synthesized nanoparticles (Fig. 2C). This result indicates the high stability of our nanoparticles. Zeta potential analysis theory states that particles in a suspension that possess a high negative or positive potential are inclined to repel one another and have no tendency to aggregate.[70] In addition, the strongly negative value of high magnitude further suggests the exceptional stability of the fabricated Ag/AgCl-NPs.[71] A TEM study was carried out to get more information about the surface morphology and size of nanoparticles. According to TEM micrographs, the average particle size was 40 ± 10 nm, with diameters ranging from 10 nm to 60 nm (Fig. 2D). Moreover, the biosynthesized nanoparticles were spherical and well dispersed even when they formed aggregates, suggesting the presence of capping agents around each nanoparticle. Additionally, the elemental composition of the biogenic Ag/AgCl nanoparticles was analyzed and confirmed using energy-dispersive X-ray spectroscopy (EDX) (Fig. 2F). According to an EDX analysis, a clear peak at 3.20 keV, is attributed to the presence of Ag metal. Another prominent peak of Cl is seen, indicating the presence of Cl in the nanoparticle structure.

Collectively, EDX and PXRD confirm the formation of Ag NPs and AgCl-NPs together.[72]

3.4 Minimum inhibition concentration

To study the inhibitory and antibacterial effects of biosynthesized Ag/AgCl-NPs, various concentrations (ranging from 1 to 12 μg mL^{-1}) of Ag/AgCl-NPs were used as antibacterial agents against pathogenic MDR bacteria *S. aureus*, *P. aeruginosa*, *A. baumannii*, and the ATCC strain of *E. coli* 25922. When compared to the control groups, the MIC of Ag/AgCl-NPs against *S. aureus*, *P. aeruginosa*, *A. baumannii*, and *E. coli* ATCC 25922 was determined to be 7 μg mL^{-1}, 7 μg mL^{-1}, 10 μg mL^{-1}, and 8 μg mL^{-1} respectively (Fig. 3). It has been illustrated that the biosynthesized Ag/AgCl-NPs have strong antibacterial efficacy against tested MDR pathogenic and ATCC bacteria at very low concentrations. These findings are in agreement with Sabzevar *et al.*,[73] who reported the antibacterial effect of biogenic Ag/AgCl-NPs on pathogenic *S. aureus* and *P. aeruginosa*, which were 25 μg mL^{-1} and 50 μg mL^{-1}, respectively. Moreover, it has been demonstrated that biologically generated AgNPs had a strong inhibitory effect against MDR *S. aureus* at 0.039 mg mL^{-1}.[74] A similar effect of AgNPs was observed in another study against 100 different strains of MDR *A. baumannii* with MIC value ranging from 4–25 μg mL^{-1}.[75] In addition, Ali *et al.*[76] showed that green-synthesized AgNPs can completely inhibit the growth of *E. coli* ATCC 25922 at a concentration of 124 ppm. Although various hypotheses have been put forth, the exact mechanism by which AgNPs exert their antimicrobial effects is still unidentified. According to different studies, the main antibacterial mechanisms of action of AgNPs are the disruption of the bacterial cell membrane and the leakage of the essential cellular biomolecules, which could be a result of elevation of the ROS level and generated oxidative stress conditions, denaturation of ribosomes, interruption of adenosine triphosphate (ATP) production, and interference in deoxyribonucleic acid (DNA) replication.[77] The small particle size and narrow particle size distribution of biosynthesized Ag/AgCl-NPs may have increased their surface area-to-volume ratio, thus increasing their interaction with bacterial cell membranes. It is established that small nanoparticles have a better ability to penetrate bacterial cell walls and produce more reactive oxygen species (ROS). The use of the biogenic approach in silver chloride nanoparticle synthesis, mediated by *Kocuria* sp., may have led to the presence of bioactive capping agents on the surface of the nanoparticles. This could have resulted in an increase in the antimicrobial potential of silver chloride nanoparticles compared to those that were chemically synthesized. The use of a composite material in AgCl-NP synthesis may have resulted in a synergistic effect on its antimicrobial potential. This is due to the sustained release of silver ions, which are well established in the literature for their ability to disrupt membrane integrity, interfere with DNA replication, and inhibit essential enzymatic processes.[78]

3.5 Histopathological study

The microscopic examination of liver tissue in the normal control group (NC) revealed well-preserved hepatocytes, exhibiting no histopathological damage, while the treated groups displayed differing levels of liver toxicity, contingent upon the dosage given (Fig. 4). The treated liver tissue in the LDNP group showed significant ($P < 0.05$) fatty changes that comprised roughly 31% of the total hepatocyte area, indicating mild fatty

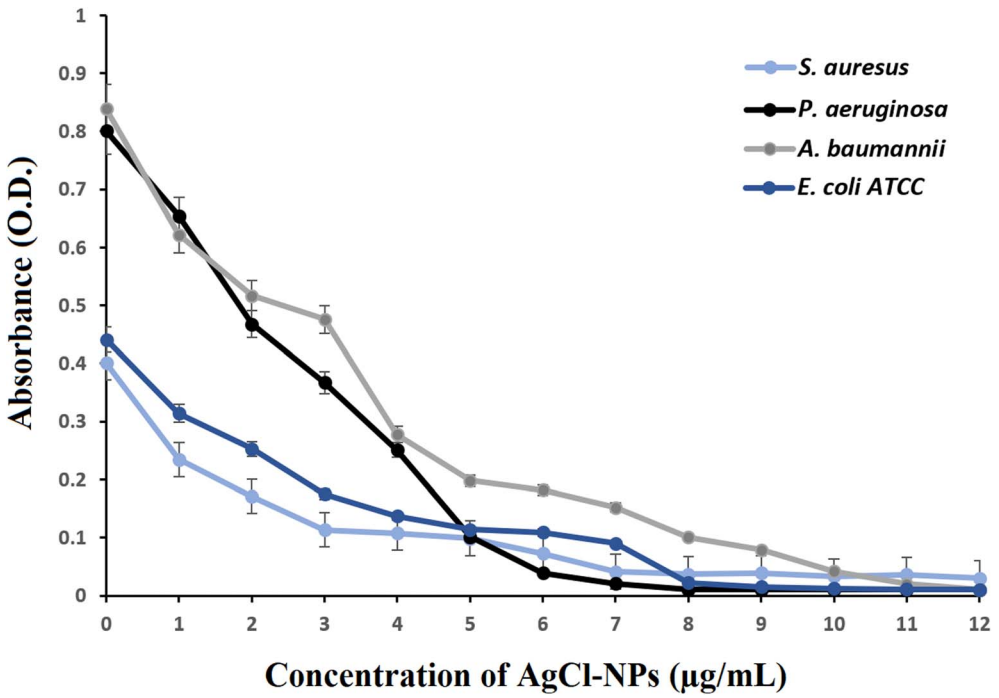

Fig. 3 Minimum inhibition concentrations of pathogenic bacteria *S. aureus*, *P. aeruginosa*, *A. baumannii*, and *E. coli* ATCC 25922 with and without exposure to Ag/AgCl-NPs.

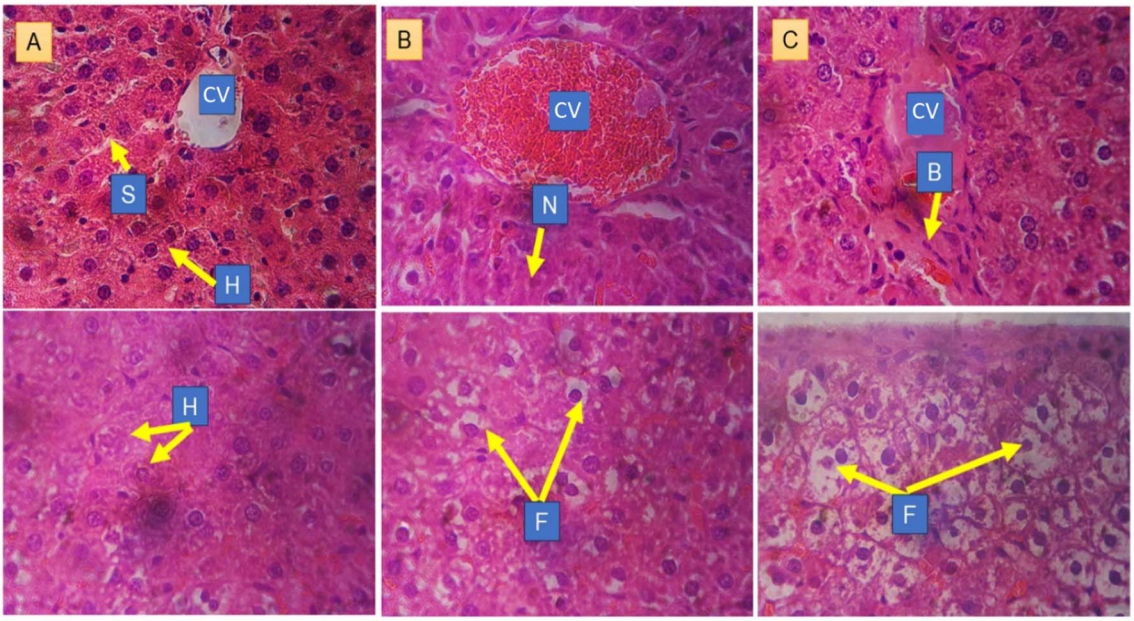

Fig. 4 Panel A: the liver tissue of the NC group, demonstrating the intact hepatic structure. The central vein (CV) is encircled by undamaged hepatocytes (H) and radiating sinusoids (S). Hepatocytes in this section exhibit no notable pathological changes, equivalent to a histopathological score of (0). Panel B: the liver tissue from the LDNP-treated group. The central vein (CV) has modest congestion, with localized regions of degenerative necrosis (N) evident. Hepatocytes display mild steatosis (F), corresponding to a histopathological score of (1). Panel C: the liver tissue from the HDNP-treated group. The central vein (CV) exhibits congestion accompanied by eosinophilic, glassy debris. Regions of degeneration, characterized by fibrosis, including active fibroblasts (B), are apparent. Hepatocytes exhibit mild steatosis (F), correlating with a histopathological score of (2). All sections were stained with hematoxylin and eosin and analysed at 400× magnification.

Table 2 Quantitative analysis of fatty infiltration and hepatic degeneration[a]

	Fatty change (% mean)	Degeneration (% mean)	Inflammation (% mean)	Score	Grade
Normal	%0[a]	%0[a]	%0[a]	0	No lesion
Low dose	%30.89[b]	%9.17[b]	%8.13[b]	1	Mild
High dose	%47.76[c]	%36.48[c]	%12.75[c]	2	Moderate

[a] Areas of fatty infiltration and degeneration were measured in square microns (μm^2). Values represent the mean of 10 measurements per group. The same letters (a, b, and c) mean no significant differences, while different letters mean significant differences.

changes (score 1). In contrast, the tissue in the HDNP treated group demonstrated more significant ($P < 0.05$) fatty changes, with approximately 48% of the hepatocyte cytoplasm impacted, indicating a substantial degree of fatty changes (score 2; Table 2). A plausible explanation for the lipid accumulation found in hepatocytes after exposure to Ag/AgCl-NPs is the simultaneous increase in plasma and hepatic triglycerides and cholesterol, along with the activation of sterol regulatory element-binding protein-1c, which promotes *de novo* lipogenesis.[79]

Regarding tissue degradation, the LDNP-treated tissue exhibited significant early-stage degeneration ($P < 0.05$), typified by hepatocytic necrosis, which constituted 9.17% of the total visible fields under a microscope and was classified as mild degeneration (score 1). In the HDNP-treated group, deterioration was more pronounced ($P < 0.05$), with tissue fibrosis evident due to fibroblast activation and fibrillar deposition. This impacted 36.48% of the visible area and was classified as mild degeneration (scoring 2; Table 2). This result aligns with a study conducted in ref. 79, which concluded that exposure to AgNPs resulted in significant hepatic pathology, marked by hepatocellular necrosis, localized tissue necrosis, granuloma development, and disruption of the normal hepatic plate structure. Additionally, significant Kupffer cell hyperplasia was noted in both treated groups ($P < 0.05$), with a more significant prevalence in the HDNP-treated group (12.75%) compared to the LDNP-treated group (8.125%) (Table 2). Kupffer cells are believed to phagocytose AgNPs upon being introduced in the liver through the bloodstream as a component of the innate immune response. This absorption results in the release of pro-inflammatory cytokines, such as TNF-α, IL-1β, and IL-6, which enhance the inflammatory response and stimulate more proliferation of Kupffer cells. The proliferation of Kupffer cells presumably signifies a compensatory mechanism to effectively eliminate nanoparticles, apoptotic hepatocytes, and cellular debris resulting from Ag/AgCl-NP -induced hepatic effects. The liver is identified as the primary location for nanoparticle

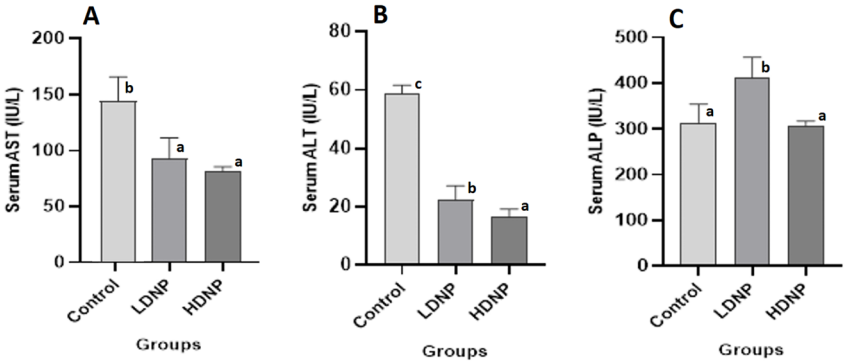

Fig. 5 Influence of low and high Ag/AgCl-NP dose administration on serum markers of hepatic function in experimental rats; (mean ± SE). (A) Serum AST levels; (B) serum ALT levels; (C) serum ALP levels. The same letters mean no significant differences, while different letters mean significant differences.

deposition.[80] The literature suggests that liver histopathological toxicity following exposure to AgNPs may result from the internalization of nanoparticles by hepatocytes, which are subsequently transported to lysosomes, where the acidic milieu facilitates their dissolution and the release of silver ions (Ag^+). These ions attach to thiol (–SH) groups on numerous proteins, disrupting their function and resulting in the production of oxidative stress and further deterioration. Simultaneously, cellular antioxidants such as glutathione and superoxide dismutase are diminished or rendered inactive while striving to mitigate the effects of Ag^+.[81] Concurrently, Ag^+ interferes with mitochondrial electron transport, resulting in electron and cytoplasmic leakage, diminished ATP generation, and the high liberation of free radicals that lead to hepatocyte necrosis, which is characterized histopathologically by cellular swelling, necrosis, and dysfunction.[82,83]

3.6 Effect of Ag/AgCl nanoparticles on liver enzymes

Serum liver enzymes AST, ALT, and ALP were analysed as indicators of hepatic function in the NC group and the LDNP- and HDNP-treated groups to assess the impact of Ag/AgCl-NPs on liver tissue in experimental rats. AST levels were the highest in the control group (145.7 U L^{-1}). Both the LDNP- and HDNP-treated groups exhibited significant ($P < 0.05$) reduction (92.48 U L^{-1} and 81.77 U L^{-1}, respectively) in comparison with the NC group (Fig. 5A). ALT, a key indicator of hepatic damage, was significantly ($P < 0.05$) reduced in both the LDNP-treated group (22.30 U L^{-1}) and the HDNP-treated group (16.48 U L^{-1}) compared to the control group (58.53 U L^{-1}). The higher dose of Ag/AgCl-NPs led to a greater ($P < 0.05$) reduction in ALT (Fig. 5B). Moreover, the lower dosage of Ag/AgCl-NPs resulted in a significant elevation ($P < 0.05$) of the ALP enzyme from 314.3 U L^{-1} to 410.5 U L^{-1}, indicating potential deleterious effects on hepatic metabolism. Nevertheless, the higher dosage of Ag/AgCl-NPs resulted in a minor decrease in serum ALP levels (305 U L^{-1}) (Fig. 5C). Our results showed that both low (10 mg kg^{-1}) and high (20 mg kg^{-1}) doses of Ag/AgCl-NPs had the ability to reduce serum liver enzyme levels in a dose-dependent manner, except for the ALP enzyme, which demonstrated that a low dose of nanoparticles can increase the enzyme level more than a high dose. These modifications in the liver enzyme levels may signify adaptive strategies employed by the animals to mitigate stress induced by exposure to Ag/AgCl-NPs. The impact of AgNPs on liver enzymes remains contentious, potentially influenced by the extent of damage inflicted by the nanoparticles on liver tissue. Consistent with our findings, Adeyemi and Adewumi.[84] demonstrated that the treatment of AgNPs in rats at concentrations of 100, 1000, and 5000 mg kg^{-1} daily for alternating periods of 7, 14, and 21 days can induce significant changes in serum and tissue levels of AST, ALT, and ALP. Upon the 100 mg kg^{-1} AgNP treatment, serum and tissue levels of AST and ALT in rats were dramatically reduced ($P < 0.05$). Conversely, AgNP treatment significantly increased ($P < 0.05$) ALP levels in rat serum and tissues. Other studies have demonstrated that AgNPs can significantly elevate the levels of liver enzymes AST and ALT in albino male rats after two weeks of treatment at varying doses, whereas ALP remained unaffected.[85,86] Belji Kangarlou *et al.*[87] utilized adult male albino Wistar rats and discovered that the administration of AgNPs at different doses (50 mg kg^{-1} and 100 mg kg^{-1}) resulted in increased levels of ALP, ALT, and AST, along with histological abnormalities in liver tissue, including severe hepatic necrosis. Although AST and ALT are traditionally considered indicative markers of hepatocellular damage in cases of increased levels, decreases in the levels of these two enzymes have been noted in response to certain metallic nanoparticles. This could be a reflection of reduced metabolic activity in the hepatocytes, reduced synthesis of these two enzymes, or reduced viable cell mass in the hepatocytes due to oxidative stress-induced cell damage.[87] In brief, the hepatic response observed in this study likely represents an equilibrium between oxidative stress induced by the nanoparticles and the liver's adaptive defense mechanisms.

4 Conclusions

Ag/AgCl-NPs were fabricated externally from the metabolite of *K. kristinae*, exhibiting a spherical morphology and an average diameter of 40 ± 10 nm. The Ag/AgCl-NPs showed significant antibacterial effectiveness against pathogenic bacteria, including *S. aureus*, *P. aeruginosa*, A. *baumannii*, and *E. coli*

ATCC 25922. Furthermore, Ag/AgCl-NPs exhibited various levels of hepatic toxicity, including steatosis, tissue degeneration such as necrosis, and hyperplasia of Kupffer cells, contingent upon the administered dosage. The alterations were minor to moderate; nonetheless, liver metabolism and function could be unaffected, as levels of liver enzymes AST and ALT were decreased, while only ALP exhibited an increase. Additional research is necessary to ascertain the impact of Ag/AgCl-NPs at varying concentrations on liver tissues, and more biochemical assays should be conducted to elucidate the toxicity of Ag/AgCl-NPs on the liver.

Ethical statement

All animal procedures were conducted in accordance with the Guidelines for the Care and Use of Laboratory Animals of the Medical Laboratory Science Department at Sulaimani Polytechnic University, and were approved by the Animal Ethics Committee of the Medical Laboratory Science Department, Sulaimani Polytechnic University.

Author contributions

Lana Mohammed: conceptualization, methodology, data curation, data analysis, writing – original draft. Mohsin A. Salih: methodology, data analysis, writing – original draft. Zana H. Ibrahim: animal husbandry, biochemical analysis, and writing. Payam B. Hassan: writing and validation. Sameera Sh Mohammad Ameen: writing – original draft, validation, methodology. Khalid M. Omer: validation, writing – review & editing. Zhinya Y. Majeed: methodology. Dalya M. Hamad: methodology, visualization. Shnyar O. Ahmed: methodology, data curation. Rayan F. Hassan: visualization, methodology. Hevy N. Hussein: data curation, methodology.

Conflicts of interest

The authors declare that there are no financial conflicts of interest.

Data availability

The data, all raw data and results, that support the findings of this study are available from the corresponding author upon request. Supplementary information (SI) is available. See DOI: https://doi.org/10.1039/d5na01052g.

References

1 M. Kolar, *Hospital Acquired Infections, Multidrug Resistant (MDR) Bacteria, Alternative Approaches to Antibiotic Therapy*, MDPI-Multidisciplinary Digital Publishing Institute, 2022.
2 S. Singh, S. Singh, M. Trivedi and M. Dwivedi, *Microb. Pathog.*, 2024, **192**, 106674.
3 S. Qin, W. Xiao, C. Zhou, Q. Pu, X. Deng, L. Lan, H. Liang, X. Song and M. Wu, *Signal Transduct. Targeted Ther.*, 2022, **7**, 199.
4 V. Šeputienė, J. Povilonis and E. Sužiedėlienė, *Antimicrob. Agents Chemother.*, 2012, **56**, 1969–1973.
5 C. Vidaillac and S. H. Chotirmall, *Expet Rev. Respir. Med.*, 2021, **15**, 649–662.
6 O. Öncül, Ö. Keskin, H. V. Acar, Y. Küçükardalı, R. Evrenkaya, E. M. Atasoyu, C. Top, S. Nalbant, S. Özkan and G. Emekdaş, *J. Hosp. Infect.*, 2002, **51**, 47–51.
7 S. A. Mekonnen, N. El Husseini, A. Turdiev, J. A. Carter, A. T. Belew, N. M. El-Sayed and V. T. Lee, *Proc. Natl. Acad. Sci. U. S. A.*, 2022, **119**, e2209383119.
8 F. N. Williams, D. N. Herndon, H. K. Hawkins, J. O. Lee, R. A. Cox, G. A. Kulp, C. C. Finnerty, D. L. Chinkes and M. G. Jeschke, *Crit. Care*, 2009, **13**, R183.
9 L. M. Weiner, A. K. Webb, B. Limbago, M. A. Dudeck, J. Patel, A. J. Kallen, J. R. Edwards and D. M. Sievert, *Infect. Control Hosp. Epidemiol.*, 2016, **37**, 1288–1301.
10 A. Zahedi Bialvaei, M. Rahbar, M. Yousefi, M. Asgharzadeh and H. Samadi Kafil, *J. Antimicrob. Chemother.*, 2017, **72**, 354–364.
11 S. Y. C. Tong, J. S. Davis, E. Eichenberger, T. L. Holland and V. G. Fowler Jr, *Clin. Microbiol. Rev.*, 2015, **28**, 603–661.
12 M. Á. Argudín, M. C. Mendoza and M. R. Rodicio, *Toxins*, 2010, **2**, 1751–1773.
13 J. Bien, O. Sokolova and P. Bozko, *J. Pathog.*, 2011, **2011**, 601905.
14 A. Adeyanju, F. Schaumburg, A. Onayade, A. Akinyoola, T. Adeyemi, O. Ugbo, R. Köck, Y. Amusa, O. Lawal and T. Adeyanju, *Antibiotics*, 2022, **11**, 1372.
15 G. L. Daikos, C. A. da Cunha, G. M. Rossolini, G. G. Stone, N. Baillon-Plot, M. Tawadrous and P. Irani, *Antibiotics*, 2021, **10**, 1126.
16 S. S. Mohammed Ameen, F. K. Algethami and K. M. Omer, *Food Chem.*, 2025, **491**, 145185.
17 A. Bedair, M. Hamed, S. Sh. Mohammed Ameen, K. M. Omer and F. R. Mansour, *Microchem. J.*, 2024, **205**, 111183.
18 S. S. Mohammad Ameen, F. K. Algethami and K. M. Omer, *TrAC, Trends Anal. Chem.*, 2025, **193**, 118489.
19 S. S. M. Ameen, F. K. Algethami and K. M. Omer, *Food Chem.*, 2025, 147452.
20 H. Bin Luo, F. R. Lin, Z. Y. Liu, Y. R. Kong, K. B. Idrees, Y. Liu, Y. Zou, O. K. Farha and X. M. Ren, *ACS Appl. Mater. Interfaces*, 2023, DOI: 10.1021/acsami.2c18691.
21 Y. Liao, T. R. Sheridan, J. Liu, Z. Lu, K. Ma, H. Yang, O. K. Farha and J. T. Hupp, *ACS Catal.*, 2023, **14**, 437–448.
22 Y. Chen, H. Xie, Y. Zhong, F. Sha, K. O. Kirlikovali, X. Wang, C. Zhang, Z. Li and O. K. Farha, *J. Am. Chem. Soc.*, 2024, **146**, 11202–11210.
23 X. Tang, L. Jia, X. Wang, S. Su, Y. Chen, X. Kong, Z. Ye, H. Xie, W. Gong and E. Du, *Angew. Chem.*, 2025, **137**, e202424859.
24 T. A. Goetjen, A. J. Kropf, S. Alayoglu, M. Delferro, J. T. Hupp and O. K. Farha, *ACS Appl. Nano Mater.*, 2022, **5**, 14961–14969.
25 K. Ma, Y. H. Cheung, H. Xie, X. Wang, M. Evangelopoulos, K. O. Kirlikovali, S. Su, X. Wang, C. A. Mirkin, J. H. Xin and O. K. Farha, *Chem. Mater.*, 2023, **35**, 2342–2352.

26 S. S. M. Ameen, F. K. Algethami, S. S. Ahmed, I. I. Ahmed, H. N. Abdelhamid and K. M. Omer, *New J. Chem.*, 2026, **50**, 1880–1891.
27 I. Ijaz, E. Gilani, A. Nazir and A. Bukhari, *Green Chem. Lett. Rev.*, 2020, **13**, 59–81.
28 P. B. Hassan, S. S. Mohammed Ameen, L. Mohammed, S. M. Muhammed Ameen and K. M. Omer, *Nanoscale Adv.*, 2024, **6**, 3801–3808.
29 E. O. Mikhailova, *J. Funct. Biomater.*, 2020, **11**, 84.
30 Y. Y. Loo, Y. Rukayadi, M.-A.-R. Nor-Khaizura, C. H. Kuan, B. W. Chieng, M. Nishibuchi and S. Radu, *Front. Microbiol.*, 2018, **9**, 1555.
31 Y. Chen, H. Xie, X. Wang, F. Sha, K. O. Kirlikovali, X. Wang, Z. Ye, X. Tang, C. Zhang and G. W. Peterson, *Angew. Chem., Int. Ed.*, 2025, **64**, e202417664.
32 K. T. Hassan, I. J. Ibraheem, O. M. Hassan, A. S. Obaid, H. H. Ali, T. A. Salih and M. S. Kadhim, *J. Environ. Chem. Eng.*, 2021, **9**, 105359.
33 S. S. Mohammed Ameen, A. Bedair, M. Hamed, F. R. Mansour and K. M. Omer, *ACS Appl. Mater. Interfaces*, 2025, DOI: 10.1021/acsami.4c17397.
34 S. S. Mohammed Ameen and K. M. Omer, *ACS Appl. Mater. Interfaces*, 2024, **16**, 31895–31921.
35 S. S. M. Ameen and K. M. Omer, *Food Chem.*, 2025, **479**, 143876.
36 S. S. M. Ameen, F. K. Algethami and K. M. Omer, *Microchem. J.*, 2025, **218**, 115235.
37 S. S. M. Ameen, F. K. Algethami, H. A. Qader, I. B. Qader, H. N. Abdelhamid and K. M. Omer, *J. Inorg. Organomet. Polym. Mater.*, 2025, DOI: 10.1007/s10904-025-04026-6.
38 S. S. M. Ameen, F. K. Algethami and K. M. Omer, *J. Inorg. Organomet. Polym. Mater.*, 2025, DOI: 10.1007/s10904-025-04091-x.
39 K. Liu, Z. Chen, T. Islamoglu, S.-J. Lee, H. Chen, T. Yildirim, O. K. Farha and R. Q. Snurr, *J. Phys. Chem. C*, 2024, **128**, 7435–7446.
40 V. Deepak, P. S. Umamaheshwaran, K. Guhan, R. A. Nanthini, B. Krithiga, N. M. H. Jaithoon and S. Gurunathan, *Colloids Surf., B*, 2011, **86**, 353–358.
41 N. Abid, A. M. Khan, S. Shujait, K. Chaudhary, M. Ikram, M. Imran, J. Haider, M. Khan, Q. Khan and M. Maqbool, *Adv. Colloid Interface Sci.*, 2022, **300**, 102597.
42 S. S. M. Ameen, F. K. Algethami and K. M. Omer, *Mater. Res. Bull.*, 2026, **199**, 114072.
43 S. S. M. Ameen, F. K. Algethami and K. M. Omer, *Microchem. J.*, 2026, **223**, 117325.
44 S. S. M. Ameen, F. K. Algethami and K. M. Omer, *Microchem. J.*, 2026, **223**, 117326.
45 S. Ying, Z. Guan, P. C. Ofoegbu, P. Clubb, C. Rico, F. He and J. Hong, *Environ. Technol. Innovat.*, 2022, **26**, 102336.
46 S. S. Mohammed Ameen, F. Algethami and K. M. Omer, *Microchim. Acta*, 2025, **192**, 146.
47 S. M. Muhammed Ameen, P. B. Hassan, S. H. Ahmed, S. S. Mohammed Ameen, S. M. Hamad and K. M. Omer, *Sci. Rep.*, 2025, **15**, 34171.
48 F. Ran, C. Li, Z. Hao, X. Zhang, L. Dai, C. Si, Z. Shen, Z. Qiu and J. Wang, *Adv. Compos. Hybrid Mater.*, 2022, **5**, 1841–1851.
49 N. Durán and A. B. Seabra, *Appl. Microbiol. Biotechnol.*, 2012, **95**, 275–288.
50 T. Jaswal and J. Gupta, *Mater. Today: Proc.*, 2023, **81**, 859–863.
51 O. Długosz, K. Szostak, A. Staroń, J. Pulit-Prociak and M. Banach, *Materials*, 2020, **13**, 279.
52 S. Chinde and P. Grover, *Mutat. Res., Genet. Toxicol. Environ. Mutagen.*, 2017, **819**, 1–13.
53 V. Savini, C. Catavitello, G. Masciarelli, D. Astolfi, A. Balbinot, A. Bianco, F. Febbo, C. D'Amario and D. D'Antonio, *J. Med. Microbiol.*, 2010, **59**, 1395–1402.
54 E. Stackebrandt, W. Frederiksen, G. M. Garrity, P. A. D. Grimont, P. Kämpfer, M. C. J. Maiden, X. Nesme, R. Rosselló-Mora, J. Swings and H. G. Trüper, *Int. J. Syst. Evol. Microbiol.*, 2002, **52**, 1043–1047.
55 M. A. Saldaña-Ruiz, J. M. Chávez-García, F. Ortiz-Alonso, C. S. Ortiz-Arce, J. E. Espinosa-Mora and J. R. Cortés-Cárdenas, *IJID Reg.*, 2023, **9**, 117–119.
56 H. Sowani, P. Mohite, H. Munot, Y. Shouche, T. Bapat, A. R. Kumar, M. Kulkarni and S. Zinjarde, *Process Biochem.*, 2016, **51**, 374–383.
57 T. Bennur, Z. Khan, R. Kshirsagar, V. Javdekar and S. Zinjarde, *Sens. Actuators, B*, 2016, **233**, 684–690.
58 M. Vaneechoutte, P. Riegel, D. De Briel, H. Monteil, G. Verschraegen, A. De Rouck and G. Claeys, *Res. Microbiol.*, 1995, **146**, 633–641.
59 Y. Namba, S. Fujisaki and T. Fukuda, *Int. J. Surg. Case Rep.*, 2020, **77**, 276–278.
60 R. Dunn, S. Bares and M. Z. David, *Ann. Clin. Microbiol. Antimicrob.*, 2011, **10**, 31.
61 L. Mohammed and H. Hamzah, *BioNanoScience*, 2024, **14**, 1021–1032.
62 N. M. S. Mahmood, A. M. R. Mahmud and I. M. Maulood, *Iraqi J. Sci.*, 2024, 4256–4270.
63 R. H. Hussein and Z. H. Ibrahim, *Kurd. J. Appl. Res.*, 2018, 107–116.
64 C. Pandit, A. Roy, S. Ghotekar, A. Khusro, M. N. Islam, T. Bin Emran, S. E. Lam, M. U. Khandaker and D. A. Bradley, *J. King Saud Univ. Sci.*, 2022, **34**, 101869.
65 K. Okaiyeto, M. O. Ojemaye, H. Hoppe, L. V Mabinya and A. I. Okoh, *Molecules*, 2019, **24**, 4382.
66 M. Sharifi-Rad and P. Pohl, *Nanomaterials*, 2020, **10**, 638.
67 M. Ider, K. Abderrafi, A. Eddahbi, S. Ouaskit and A. Kassiba, *J. Cluster Sci.*, 2017, **28**, 1051–1069.
68 J. Bai, Y. Li, M. Li, S. Wang, C. Zhang and Q. Yang, *Appl. Surf. Sci.*, 2008, **254**, 4520–4523.
69 F. Gui, W. Mo, X. Guo, F. Cao, T. Zhai, C. Hong, X. Guan, B. Huang and X. Pan, *Adv. Agrochem*, 2023, **2**, 88–96.
70 S. Roy, T. Mukherjee, S. Chakraborty and T. K. Das, *Dig. J. Nanomater. Biostruct.*, 2013, **8**, 197–205.
71 P. P. Dutta, M. Bordoloi, K. Gogoi, S. Roy, B. Narzary, D. R. Bhattacharyya, P. K. Mohapatra and B. Mazumder, *Biomed. Pharmacother.*, 2017, **91**, 567–580.
72 M. T. Yassin, A. A.-F. Mostafa, A. A. Al-Askar and F. O. Al-Otibi, *Crystals*, 2022, **12**, 603.
73 A. H. Sabzevar, G. R. Hashemitabar, M. Rad and J. Vatandoost, *Braz. Arch. Biol. Technol.*, 2021, **64**, e21210010.

74 N. A. Al-Dhabi, A.-K. Mohammed Ghilan and M. V. Arasu, *Nanomaterials*, 2018, **8**, 279.
75 H. F. Hetta, I. M. S. Al-Kadmy, S. S. Khazaal, S. Abbas, A. Suhail, M. A. El-Mokhtar, N. H. A. Ellah, E. A. Ahmed, R. B. Abd-Ellatief and E. A. El-Masry, *Sci. Rep.*, 2021, **11**, 10751.
76 Z. H. Ali and A. H. Al-Fatlawi, *Results Eng.*, 2023, **17**, 100988.
77 I. X. Yin, J. Zhang, I. S. Zhao, M. L. Mei, Q. Li and C. H. Chu, *Int. J. Nanomed.*, 2020, 2555–2562.
78 A. K. Yegon, J. A. Oyetade, S. G. Mtavangu, M. J. Rwiza and R. L. Machunda, *Discover Nano*, 2025, **20**, 120.
79 L. Wen, M. Li, X. Lin, Y. Li, H. Song and H. Chen, *Front. Bioeng. Biotechnol.*, 2022, **10**, 912178.
80 Y. S. Kim, J. S. Kim, H. S. Cho, D. S. Rha, J. M. Kim, J. D. Park, B. S. Choi, R. Lim, H. K. Chang and Y. H. Chung, *Inhal. Toxicol.*, 2008, **20**, 575–583.
81 S. K. Das, K. Sen, B. Ghosh, N. Ghosh, K. Sinha and P. C. Sil, *World J. Hepatol.*, 2024, **16**, 566.
82 M. R. Almofti, T. Ichikawa, K. Yamashita, H. Terada and Y. Shinohara, *J. Biochem.*, 2003, **134**, 43–49.
83 S. Arora, J. Jain, J. M. Rajwade and K. M. Paknikar, *Toxicol. Lett.*, 2008, **179**, 93–100.
84 O. S. Adeyemi and I. Adewumi, *Int. Sch. Res. Not.*, 2014, **2014**, 196091.
85 J. Cheraghi, E. Hosseini, R. Hoshmandfar, R. Sahraei and A. Farmany, *Adv. Environ. Biol.*, 2013, 116–123.
86 Z. Falah and A. M. Rabee, *Iraqi J. Sci.*, 2022, 4195–4204.
87 M. Belji Kangarlou, A. Khavanin, F. Nadri, Z. Goodarzi, E. Karami, A. Rashidy-Pour, M. Kiani and R. Hashemi Habybabady, *Toxicol. Ind. Health*, 2024, **40**, 206–219.